Colloids and Surfaces A: Physicochemical and Engineering Aspects 632 (2022) 127743

Contents lists available at ScienceDirect

Colloids and Surfaces A: Physicochemical and Engineering Aspects

journal homepage: www.elsevier.com/locate/colsurfa

Design of a pDNA nanocarrier with ascorbic acid modified chitosan coated on superparamagnetic iron oxide nanoparticles for gene delivery

Mehri Karimi Jabali [a], Ali Reza Allafchian [b,d,*], Seyed Amir Hossein Jalali [c,d], Hamideh Shakeripour [a], Rezvan Mohammadinezhad [d], Fahime Rahmani [b]

[a] Department of Physics, Isfahan University of Technology, Isfahan 84156–83111, Iran
[b] Research Institute for Nanotechnology and Advanced Materials, Isfahan University of Technology, Isfahan 84156–83111, Iran
[c] Department of Natural Resources, Isfahan University of Technology, Isfahan 84156–83111, Iran
[d] Research Institute for Biotechnology and Bioengineering, Isfahan University of Technology, Isfahan 84156–83111, Iran

HIGHLIGHTS

- Ascorbic acid modified chitosan was coated on Fe_3O_4 nanoparticles as pDNA nanocarriers
- The nanoparticles were characterized by FE-SEM, FT-IR, XRD, VSM, and DLS
- The MTT assay confirmed biocompatibility of the nanocarriers to Vero and EPC cells
- The loaded pDNA contents were released successfully in intestinal environment

GRAPHICAL ABSTRACT

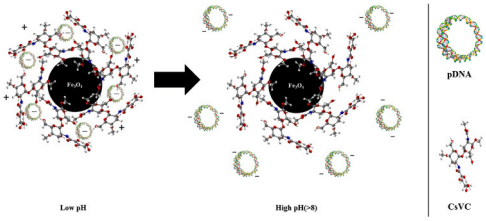

ARTICLE INFO

Keywords:
Gene delivery
Plasmid DNA
Iron oxide nanoparticle
Chitosan
Ascorbic acid

ABSTRACT

Hypothesis: Among various approaches of gene delivery, there is a growing interest in oral administration of plasmid DNA (pDNA) as one of the safest and most straightforward vaccination methods. Inclusion of chitosan is expected to prevent pDNA degradation in gastric environments and contribute to releasing it in target intestinal fluids.

Experiments: In this paper, ascorbic acid-modified chitosan is used as a biomolecular coating on superparamagnetic iron oxide nanoparticles (SPION) to serve as a pDNA nanocarrier. The nanoparticles are studied by FE-SEM, DLS, zeta potential, FT-IR spectroscopy, XRD, and VSM. The pDNA release in a simulated intestinal environment is measured by agarose gel electrophoresis. The cytotoxicity of the nanoparticles is evaluated by MTT assay using epithelial Vero and EPC cells.

Findings: Results show that the nanocarriers are formed spherically with a mean hydrodynamic diameter of 100 nm and zeta potential of + 25 mV. The nanocarrier gastric stability is confirmed by treating with DNase I test. The results show that the pDNA release is promising and amounts to 45% after 48 h. MTT assay results show that the SPION@CsVC nanocarriers are biocompatible to Vero and EPC cell lines. It is found that chitosan can effectively shield the pDNA in the extremely acidic gastric environment, yet allows it to be released when passing through the target alkaline intestinal tissue. In other words, chitosan is presented as an effective biopolymer for application in non-viral vectors for gene delivery through a facile oral route.

* Corresponding author at: Research Institute for Nanotechnology and Advanced Materials, Isfahan University of Technology, Isfahan 84156–83111, Iran.
E-mail address: allafchian@cc.iut.ac.ir (A.R. Allafchian).

https://doi.org/10.1016/j.colsurfa.2021.127743
Received 13 July 2021; Received in revised form 9 October 2021; Accepted 12 October 2021
Available online 16 October 2021

1. Introduction

The significance of gene delivery is elucidated by the advantages it has to offer over conventional medical procedures. Gene therapy can offer hope to many patients suffering from serious diseases such as genetic disorders, immunodeficiency, hematologic disorders and cancer that may be challenging for traditional medicine [1–3]. As a critical stage in gene therapy, gene delivery can potentially contribute to cancer treatment by tackling the origin of the disease, i.e. DNA damage that leads to abnormal growth signals and tumor generation. In case of brain tumors, gene delivery is preferred due to potential unrecoverable brain injuries caused by surgical treatments. Moreover, treatment of primary brain tumors such as glioblastoma by conventional drugs is significantly limited due to effects of blood brain barrier, immunosuppressive microenvironment of tumors and developed resistance to drugs [4]. Gene therapy for cancer treatment is envisioned as a promising solution to overcome limitations of current anticancer strategies by genetic approaches such as administering tumor suppressor genes, suicide genes and inhibiting the oncogene activity by RNA interference [5].

Naked DNA molecules, that are negatively charged, not only are fragile and degradable in presence of proteolytic enzymes and serum proteins [6] but also are unable to cross the cell membrane. Therefore, successful delivery of genes to the cytosol requires overcoming several extracellular and intracellular barriers including enzymatic degradation and cytoplasmic cellular membrane [7,8], and development of effective and safe vectors is essential for gene delivery applications; in particular, the vector would help the genes enter the cellular space and mediate their effect. As a result, success of gene therapy depends to a large extent on the vector type for effective gene transfection to occur [9,10].

Generally, these carriers or vectors can be divided into viral and non-viral types [11]. Although viral vectors have high transfer efficiency, but the occurrence of toxicity, immunogenic problems, and enzymatic degradation make them perilous [8]. In order to solve or mitigate the problems, non-viral vectors have been considered in medical research centers to facilitate gene transfer [12,13]. The ease of production, manipulation, storage, and shipping has made it more enthralling to consider plasmids as potential candidates [14]. However, the low transfection efficiency of plasmids is challenging. To increase the efficiency of pDNA transfer, different carriers are extensively investigated. These carriers, including polymers (polyplexes), lipids (lipoplexes), and inorganic materials (e.g. calcium phosphate), are able to bond with pDNA through covalent or noncovalent interactions [15,16]. While the candidate polymers for pDNA loading are less immunogenic and toxic than cationic lipids, they are more stable, making them proper alternatives for viral and lipid transfer methods. Structural variation, compatibility, and possibility of covalent or ionic bonding with components for gene expression offer interesting opportunities [11,17]. Various cationic polymers have been optimized for transferring DNA since fifty years ago [18]. Because of their unique structural properties, natural polymers receive significant attention in this area [19]. Chitosan is one of the natural polymers studied by many researchers and its derivatives make it a more functional compound compared to other non-viral nanocarriers [20–22].

Chitosan is a biocompatible, biodegradable linear polysaccharide with a high level of cationic potential [23] with remarkable biomedical applications including drug delivery [24,25]. This biopolymer is obtained from deacetylation of chitin, which is nontoxic, easily accessible, and inexpensive. Chitosan, with its cationic polyelectrolytic nature, can provide a strong electrostatic interaction with anionic DNA and establish sustained compounds to prevent DNA destruction [26,27]. High molecular weight chitosan (100–400 kDa) can form a highly stable combination with DNA [28,29]. However, by increasing molecular weight, its solubility in aqueous environments decreases [30]. Besides, the weakness of chitosan in buffering capacity affects its endosomal escape [31]. To resolve the dissociation rate of pDNA and endosomal obstacles, different functional groups can be introduced into amine, amide, or hydroxyl groups of chitosan [32]. Ascorbic acid, a ketolactone containing four hydroxides and a lactone, plays the role of an effective antioxidant in biological systems. Because of its biochemical functions, in particular, the antiviral and antitumor activity, ascorbic acid attracts great interest in the medical and biological studies [33]. However, its use is limited due to its physical and chemical instability. In low pH levels, cationic amino acid branches in chitosan and anionic hydroxyl branches of ascorbic acid are activated and linked [34]. In this case, also, to increase the solubility of chitosan and the structural stability of ascorbic acid, the antioxidant activity of the mixture increases as compared to both materials [35]. To pass extracellular barriers and escape endosomal degradation, pDNA molecules are compressed into polymeric nano/microparticles to suit a proper cellular uptake [36,37]. A wide range of nano-based non-viral carriers are efficiently designed, and intelligent carriers are continuously optimized to control the fate of DNA molecules [38,39]. However, the inability to reach the target cells is still problematic. For this reason, nanoparticles are equipped with a magnetic core to be dirigible [40,41]. Due to their unique properties such as superparamagnetic nature, operative surface, high surface-to-volume ratio, low toxicity, and ease of manipulation using magnetic fields, iron oxide nanoparticles have found many potential applications in biomedicine [42–46]. The cellular uptake of SPION is also investigated by researchers, and the results show their precedence to non-magnetic nanocarriers [47].

The present study is concerned with constructing biocompatible magnetic nanocarriers with low toxicity and high efficiency for transfer and delivery of pDNA through oral administration. The nanocarriers are characterized by Fourier-transform infrared spectroscopy (FT-IR), alkaline titration, X-ray diffraction (XRD), energy dispersive spectroscopy (EDS), dynamic light scattering (DLS), zeta potential measurement, and vibrating sample magnetometry (VSM). The nanoparticles are also studied using a field emission scanning electron microscope (FE-SEM). By exposing the loaded nanocarriers to simulated gastric intestinal environments, various properties of the samples including stability and pDNA release in vitro are examined by UV spectrophotometry, DNase I test, and agarose gel electrophoresis. Eventually, the cytotoxicity of the nanocarriers is examined by MTT assay on Vero and endothelial progenitor cells (EPC).

2. Materials and methods

2.1. Materials

Iron (II) sulfate (99.9%), sodium sulfate (99.9%), and sodium hydroxide (99.9%) were purchased from Merck, Germany. Acetic acid (99.9%), Iron (III) nitrate (99.9%), and dimethyl sulfoxide (DMSO) (99.9%) were purchased from Scharlau, Spain. Pure chitosan with an average molecular weight of 70 kDa and deacetylation of 98% was purchased from Sigma-Aldrich, the US. L-Ascorbic acid was purchased from Appli-Chem, Germany. 3-(4,5-Dimethylthiazol-2-yl)− 2,5-diphenyl tetrazolium bromide (MTT) was purchased from Solar Bio, China. Fetal bovine serum (FBS) was supplied from Gibco, Singapore. EPC (CRL-2872) and Vero (CCL-81) cells were provided from ATCC, the US. The pDNA (3.1(+)) was extracted from *E. coli* (DH5α) by rapid alkaline lysis. All chemicals were used as received without further purification.

2.2. Synthesis of polymer (CsVC)

Synthesis of ascorbic acid-modified chitosan (CsVC) was attempted initially by preparing a 0.7% w/v chitosan solution in acetic acid (1% w/v). The pH of the chitosan solution was adjusted to pH= 5.0 by adding sodium hydroxide (1.0 M). Next, 60.0 mg ascorbic acid was added to the solution and stirred for 24 h. The solution was purified by dialysis against DI water using a 12 kDa dialysis membrane in 3 days. Finally, the purified polymer was freeze-dried and stored at room temperature.

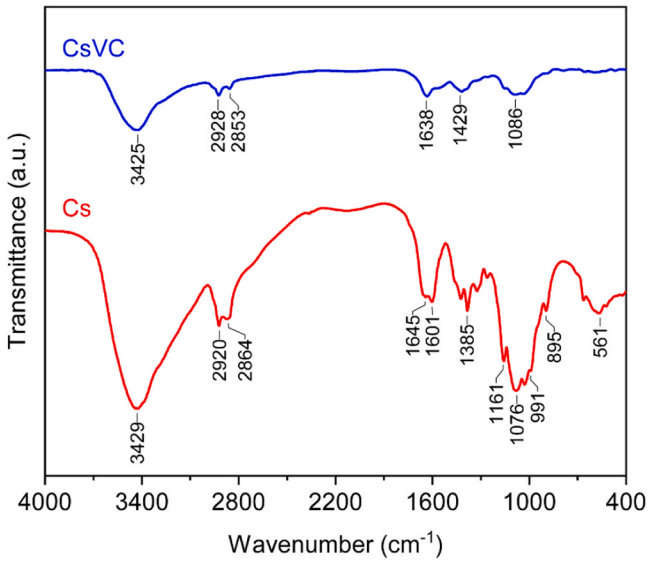

Fig. 1. FT-IR spectra of the untreated chitosan (Cs) and ascorbic acid-modified chitosan (CsVC).

Table 1
Degree of deacetylation (DD) of untreated and ascorbic acid modified chitosan.

Sample	1st DD (%)	2nd DD (%)	3rd DD (%)	Mid DD (%)
Cs	97.40	98.05	98.06	97.80
CsVC	71.70	71.80	71.50	71.70

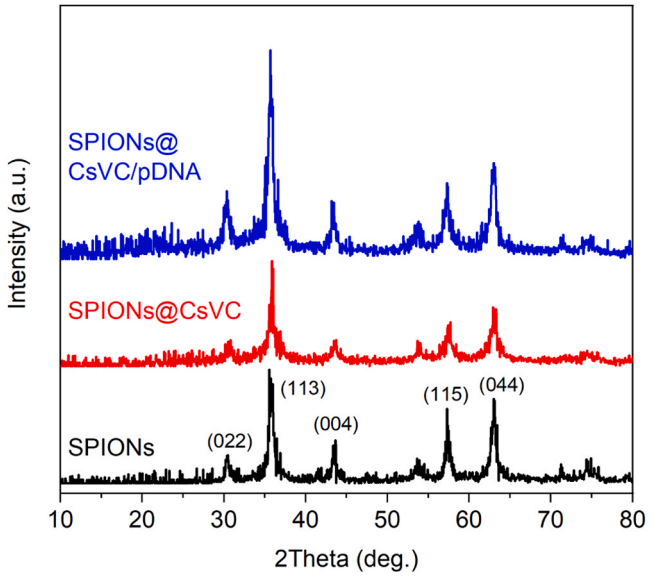

Fig. 2. XRD patterns of bare SPION, SPION@CsVC, and the final nanocarriers (SPION@CsVC after crosslinking).

Fig. S1 shows a schematic illustration of chemical modifications during CsVC preparation.

2.3. Synthesis of chitosan coated SPION

The synthesis of coated SPION (SPION@Cs and SPION@CsVC) was done via a modified in-situ co-precipitation method (Fig. S2) [48]. Briefly, solutions of 0.1% w/v Cs and CsVC in acetic acid (1% w/v) were prepared and the pH = 4.5 adjustment was done by sodium hydroxide

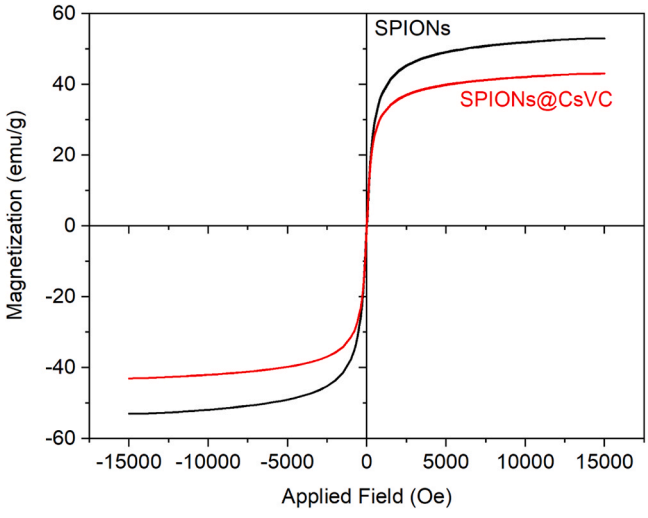

Fig. 3. Magnetization curves of bare SPIONs and the nanocarriers.

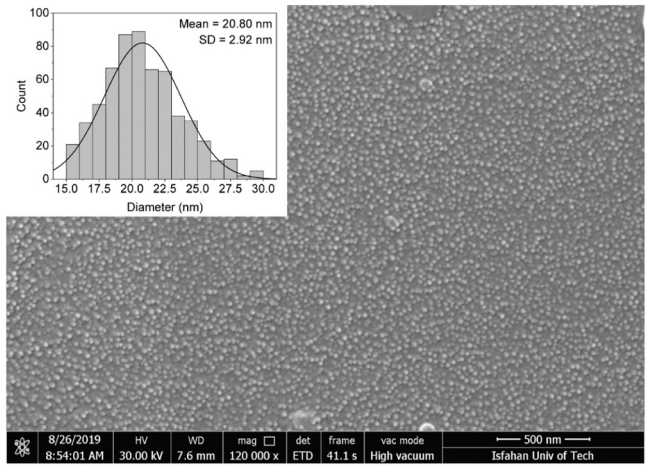

Fig. 4. FE-SEM image of the nanocarriers with their particle size distribution (Inset).

(1.0 M). Then, the iron salts were added such that the Fe(II):Fe(III) molar ratio was set as 1:1 and the polymer to iron salts ratio was adjusted to 0.05 (w/w). To obtain SPION, the solutions were titrated (1 mL/min) with sodium hydroxide as an alkaline precipitator (1.0 M) until pH = 11 was reached. The black sediments were collected with a strong magnet and washed several times with DI water by centrifugation. Finally, SPION@Cs and SPION@CsVC nanoparticles were dried overnight and kept under Ar environment.

2.4. Loading of pDNA and alkaline titration analysis

To load pDNA on SPION@Cs and SPION@CsVC, dispersions of coated SPION were prepared in 50.0 mM acetic acid buffer. Then, 3.0 μg of pDNA was added to every milliliter of the dispersions. Accordingly, each sample unit is defined as 250 μL dispersion that contains 125 μg of coated SPION and sodium sulfate as an ionic crosslinker.

The degree of deacetylation (DD) of CsVC was determined by alkaline titration method. Briefly, the degree of deacetylation can be calculated by Eq. (1).

$$DD(\%) = \frac{\varphi}{\frac{W - \frac{161}{204}\varphi}{} + \varphi} \times 100 \quad (1)$$

where Φ is

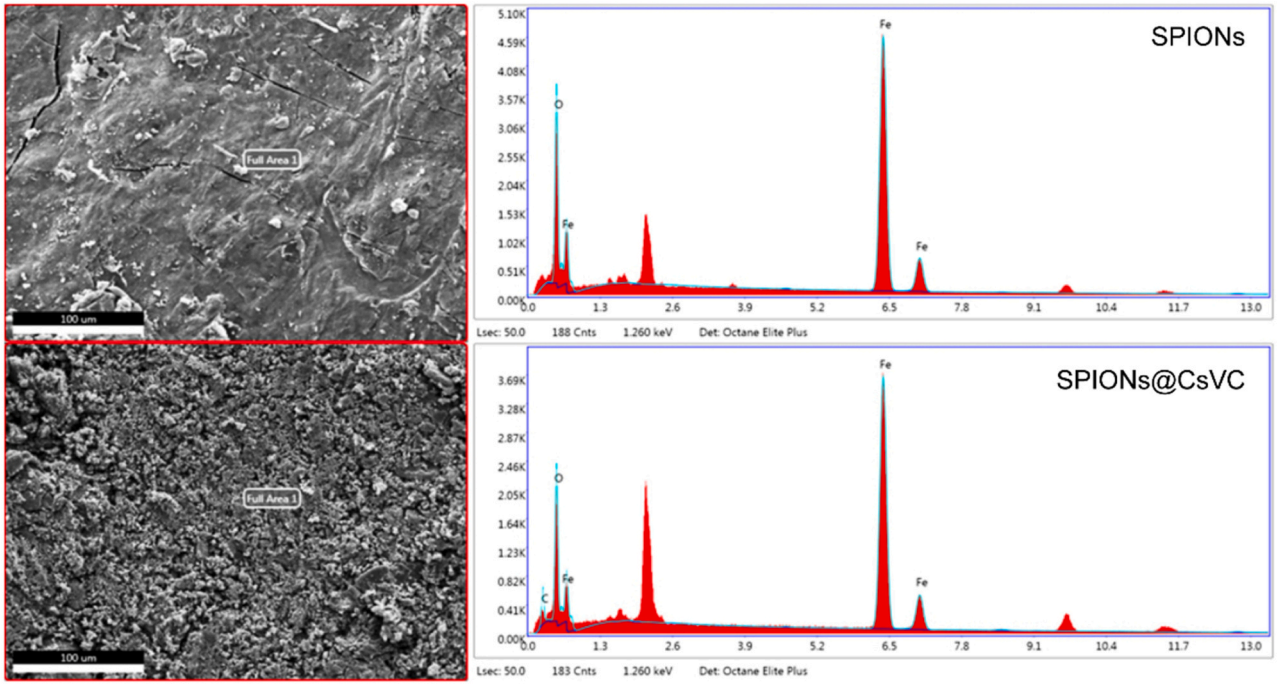

Fig. 5. EDS map of bare SPIONs and the nanocarriers. The scale bars are 100 μm.

$$\Phi = \frac{(N_A \times V_A) - (N_B \times V_B)}{100} \quad (2)$$

In Eq. (2), N_A and N_B are concentrations of standard acid and alkaline solution that were applied during titration and V_A and V_B represent their volumes. It is noted that the calculation was done three times.

2.5. Characterization

To investigate the functional groups and chemical bonds, FT-IR spectra of the untreated and ascorbic acid-modified chitosan samples as well as bare and coated SPION were obtained in the range of 400–4000 cm^{-1} by a Bruker Tensor 27 instrument. To study the structural properties of the samples, XRD patterns of the nanoparticles were obtained in different levels of synthesis using a PANalytical X'Pert PRO diffractometer. EDS maps of the nanoparticles were taken to investigate their chemical composition. The FE-SEM image of the nanocarriers was taken in high vacuum by a Quanta FEG 450 instrument together with an EDS analysis. The mean size of nanoparticles was calculated by measuring the size of 600 nanoparticles, which were selected randomly. The hydrodynamic size and zeta potential of the nanoparticles were measured at ambient temperature by a Horiba SZ-100 instrument. The magnetic behavior of the nanoparticles was determined by VSM in the range of 0–15000 Oe.

Loading of pDNA on nanoparticles was investigated using UV spectrophotometry, DNase I test, and agarose gel electrophoresis. Stability and release of nanoparticles in vitro were tested using simulated gastric fluid (SGF, pH = 2), and simulated intestinal fluid (SIF, pH = 9), respectively. The stability of the nanoparticles refers to their resistance to degradation in gastric environments. The SGF was designed using HCl (1.0 M) to examine stability in pH = 2. The SIF includes a complex of dihydrogen sodium phosphate (150 mM), sodium chloride (400 mM), and imidazole (50 mM), which have reached the optimum volume in the tris buffer (50 mM). This solution also has a highly stabilized pH at 8–10 [49]. To detect the pDNA loaded on nanoparticles, UV spectrophotometry was carried on the nanoparticle suspensions by a NanoDrop pico 200 spectrophotometer.

2.6. DNase I test and electrophoresis

To detect the possible pDNA attachment on the surface of nanocarriers, DNase I test was performed on the samples that were investigated by UV spectrophotometry. Briefly, DNase I was added to the nanoparticles and then activated at 37 °C. The nanoparticles were then dispersed and incubated for about an hour, so the enzyme can act and destroy all plasmids attached on the surface of nanoparticles. Next, the enzyme was inactivated by EDTA buffer (25 mM) and the nanoparticles were collected by centrifugation (10000 rpm) and finally dispersed in sterile water.

To obtain the amount of pDNA released from nanoparticles when exposed to SGF and SIF, agarose gel electrophoresis was carried out on the samples after UV spectrophotometry and DNase I tests. The samples were run on 0.7% w/v agarose gel at 100 V for 40 min. The released pDNA was visualized by staining with ethidium bromide. The release rate of pDNA loaded on the carriers was calculated by the Korsmeyer-Peppas model [50] as described in Eq. (3).

$$\frac{M_t}{M_f} = kt^n \quad (3)$$

In this model, M_t/M_f is the function of drug release, k denotes the rate constant, and n shows the release exponent.

2.7. MTT assay

The cytotoxicity of nanoparticles for both homoeothermic (EPC) and poikilothermic (Vero) cells was evaluated by MTT assay. The MTT method is based on the colorimetric change of yellow tetrazolium MTT to purple crystalline formazan during the mitochondrial activity of living cells. The MTT assay was carried out in 96-well plates. Initially, the plates containing living cells were prepared with a density of 2×10^4 cells/well. Then, 100 μL of DMEM medium containing 10% FBS serum was added to the cells. The cells were incubated under 88% humidity at 37 °C for 24 h. The SPION@CsVC nanoparticles in concentrations of zero (control), 0.1, 1 and 10 μg/mL were added to the cells. The cells were treated with the nanocarriers for 12, 24, and 72 h and washed with PBS. The MTT dye was dissolved in PBS (0.5% w/v). In the next step, around

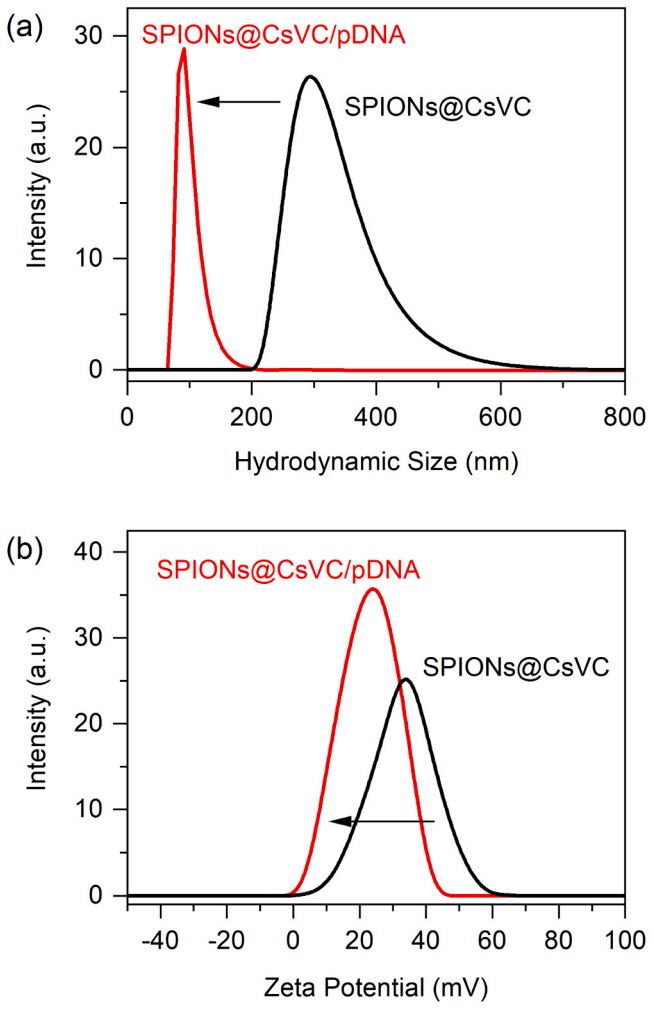

Fig. 6. (a) The hydrodynamic size and (b) zeta potential of SPION@CsVC and the nanocarriers.

100 μL DMEM medium (serum-free) containing 10 μL MTT was added to each well. The cells were incubated at 37 °C for 4 h. By adding 100 μL DMSO, the formazan crystals were dissolved, and the entire contents of the wells were transferred to new wells before reading by ELIZA reader at 570 nm [51].

3. Results and discussion

3.1. FT-IR analysis

The FT-IR spectra can reveal information about the chemical bonds and functional groups in the samples. As plotted in Fig. 1, the peaks appeared at 1080, 1645, 2915, and 3425 cm^{-1} refer to the chitosan skeleton in both spectra. The broad peak appeared at 3425 cm^{-1} is related to strong tensile vibrations of C-OH. It overlaps with the N-H amide peak as a result of reaction with the amide compounds, which is evident in the region of about 3300 cm^{-1}. The bands observed in 2860 cm^{-1} and 2926 cm^{-1} are related to the vibrations of C-H. The peak emerged at 1645 cm^{-1} is related to C═O amide vibrations. The obtained spectra were compared with previous studies. The similarity between spectra indicates that the linkage of ascorbic acid to chitosan is established successfully.

3.2. Alkaline titration

The results of alkaline titration are shown in Table 1. The change in the percentage of deacetylation from 98% to 72% also indicates the blockage of amine groups in the sample structure due to association with the hydroxy group of ascorbic acid. This result is in agreement with the obtained FT-IR results. Lower DD is expected to improve the ability of biopolymers for gene delivery applications.

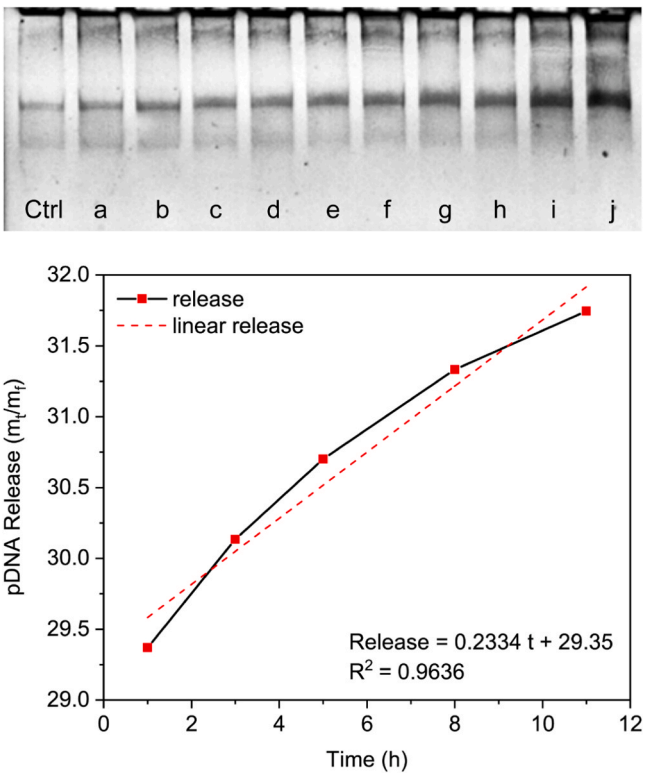

Fig. 7. Agarose gel electrophoresis of the release of nanocarrier at times of (a) 3, (b) 5, (c) 8, (d) 11, (e) 24, (f) 36, (g) 48, (h) 56, (i) 64 and (j) 80 h after exposure to SIF. *Below:* Diagram of pDNA release from nanocarriers during 12 h of incubation in SIF.

3.3. XRD and VSM analysis

The XRD spectra of nanoparticles in Fig. 2 confirms the formation of Fe_3O_4 spinel structure during various synthesis levels of the nanocarriers. The characteristic peaks at $2\theta = 30.19°$, 35.56°, 43.22°, 57.17°, and 62.78° are related to (022), (113), (004), (115) and (044) crystallographic planes of the pure cubic lattice structure (JCPDS No. 3–0863) for bare and coated SPION. As inferred from the XRD data, the process of synthesis has no significant impact on the quality of nanocarrier cores. The VSM results of nanoparticles illustrated in Fig. 3 show their superparamagnetism with a saturation magnetization of 52 emu/g for bare SPION and 46 emu/g for the nanocarriers. It is clear that the reduction of M_s for coated nanoparticles is related to dead spin layers of the shell.

3.4. FE-SEM, EDS, hydrodynamic size and zeta potential

The FE-SEM image of the nanocarriers shows that the mean particle size is 21 ± 2.917 nm. The particles are formed homogeneously in almost spherical shapes (Fig. 4). The EDS spectra of bare and coated SPION and the nanocarriers were obtained to investigate the constituent elements. As shown in Fig. 5, the elemental composition of bare SPION includes Fe and O. As expected for coated SPION (data are not shown) and the nanocarrier, carbon peaks are also evident in the data in addition to the peaks of Fe and O. The hydrodynamic diameter of SPION@CsVC particles and the nanocarriers dispersed in 50 mM acetic acid buffer in the concentration of 50 μg/mL were measured (Fig. 6**(a)**).

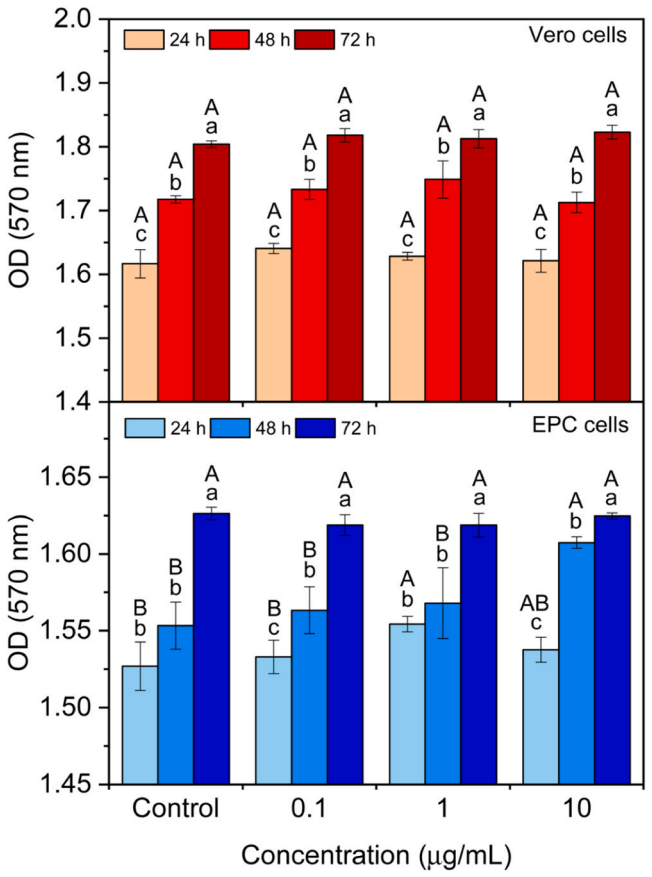

Fig. 8. MTT results of Vero and EPC cells treated by the nanocarriers after 24, 48, and 72 h of cell seeding. Different capital letters indicate significant differences between different samples on the same time period ($P < 0.05$) and different small letters represent significant differences between different times of the same sample ($P < 0.05$).

The size was calculated at pH= 5.0 to estimate the hydrodynamic size of nanoparticle in endosomal entrance. The hydrodynamic diameter of SPION@CsVC particles was 302 nm, while it was 100 nm in case of the final nanocarriers. The zeta potential values of SPION@CsVC before and after the pDNA loading were determined as + 32 and + 25 mV, respectively (Fig. 6**(b)**). It is found in literature that the minimum zeta potential of ± 20 mV is desirable for cellular uptake [52].

3.5. Loading, stability, and release tests

The gel electrophoresis image in Fig. 7 illustrates the pDNA released from nanocarriers that remained at room temperature overnight. The release of pDNA from nanocarriers is rapid within the first hour of incubation in the SIF, followed by a slow, steady release up to 50 h of exposure, and then the release rate increases again. This result is in a good conformation with previous studies. The initial rapid release is due to the release of pDNA from the polymeric layers. The subsequent release of deep pDNA occurs at a slow and uniform rate. Based on the exponent of time, this behavior can shift to one of the famous drug release models, i.e. the Korsmeyer-Peppas model. The increase at the end of release is also due to the decomposition and degradation of the polymer in its release buffer. The R^2 value was obtained as 0.96 by fitting the release curve on this model (Fig. 7). The exponent of time is the one that shows time-independent release. Therefore, the model can shift to the zero-order release mechanism.

Similar to the pDNA system presented here, encapsulation of other genetic materials, e.g. small interfering RNA (siRNA), in a chitosan-based delivery system can be beneficial with respect to selective release in basic conditions. In a study on Survivin (SVN), which is a target in cancer therapy, an effective siRNA/Cs complex with 200 nm particles has suppressed the growth of prostate cancer thanks to an improved cellular uptake by the Cs-based nanoparticles, while remaining completely stable in acidic and neutral conditions [53].

3.6. MTT assay

The MTT assay was used to assess the biocompatibility and toxicity of SPION@CsVC/pDNA nanoparticles on fibroblast cells. As illustrated in Fig. 8, there is no negative impact on viability of both cell lines by the presence of nanocarriers. There is also no significant difference among groups of Vero cells at the same time. On the other hand, the terms are somewhat different for EPC cells. The growth behavior of cells apparently remains the same during 72 h of culture. The low cytotoxicity of plasmid/chitosan complexes are also illustrated in other studies. While protection of plasmids is approved by a DNase I assay in a previous study on plasmid/chitosan formulation, the MTT results confirm a negligible cytotoxicity on 293 T cells [54]. In another study on arginine-modified chitosan complexed with liposome systems, it is demonstrated by MTTassay performed 48 h after transfection that the nanoparticles are non-toxic to HEK293 T cells [55]. In another formulation consisting of iron oxide nanoparticles conjugated with chondroitin sulfate/polyethylenimine copolymers for pDNA delivery, the results indicate an almost non-toxic interaction of the nanoparticles with 293 T, CRL5802, and U87-MG cells [56]. Delivery of a DNA vaccine for Asian sea bass through the oral route using chitosan–tripolyphosphate nanoparticles has shown that the formulation is poorly citotixic to sea bass kidney cell line (SISK) [57]. With the established biocompatibility of chitosan as a natural polymer [58], it is then strongly approved by MTT results that the SPION@CsVC could be considered as a safe non-viral vector for delivery of pDNA through the gastrointestinal system.

4. Conclusion

In this study, biocompatible superparamagnetic iron oxide nanoparticles (SPION@CsVC) with a mean size of about 21 nm have been successfully synthesized by an in-situ co-precipitation method and coated with ascorbic acid modified chitosan to function as a carrier of pDNA through the gastrointestinal system. Clinically, this method presents a prospetive application in pDNA delivery through the gastrointestinal pathway to induce vaccination or treatment of large populations of fish. A remarkable pDNA protection and release behavior was observed in simulated gastric and intestinal environments in vitro. The FT-IR spectroscopy showed that chitosan and ascorbic acid are linked successfully. The XRD analysis showed that the synthesis process did not change the core structure. The results of VSM analysis confirmed the superparamagnetism of bare SPIONs with a saturation magnetization of about 52 emu/g. It was found that in presence of chitosan, the surface charge of cores would increase in magnitude. The pDNA loading is facilitated due to the electrostatic interactions with nanoparticles. The loading and stability of pDNA loading were optimal at pH = 4.3, and the release process was about 50% at pH = 9 after 96 h. The presented technique addresses the limitations such as cytotoxicity in delivering pDNA to the desired target of intestinal tissue [37]. However, the findings of this study suggest that tailoring the nanocarrier properties by functionalization and chitosan coating could effectively benfit the delivery by protecting the loaded DNA when exposed to the gastric fluid and selectively releasing it at the target intestinal site, thus contributing to the design of effective DNA delivery systems.Additionally, SPIONs as biocompatible particles would contribute to the integrity of the nanoparticles and magnetically assisted transfection of genes through the oral route. Therefore, combination of these features in a single nanosystem is a primising method for non-viral pDNA delivery compared to previous studies.

CRediT authorship contribution statement

Mehri Karimi Jabali: Methodology; Investigation; Formal analysis; Visualization; Writing - original draft. **Ali Reza Allafchian**: Project administration; Supervision; Conceptualization; Writing - review & editing; Resources. **Seyed Amir Hossein Jalali**: Supervision; Conceptualization; Writing - review & editing, Resources. **Hamideh Shakeripour**: Supervision; Conceptualization; Writing - review & editing; Resources. **Rezvan, Mohammadinezhad**: Methodology; Investigation; Formal analysis; Visualization. **Fahime Rahmani:** Methodology; Investigation; Formal analysis; Visualization.

Funding

This work was supported by the Research Institute for Nanotechnology and Advanced Materials (RINAM) at Isfahan University of Technology, Iran.

Declaration of Competing Interest

The authors declare that they have no known competing financial interests or personal relationships that could have appeared to influence the work reported in this paper.

Acknowledgements

The authors wish to thank the Iranian Vice-President for Science and Technology and Research Institute for Biotechnology and Bioengineering for supporting this work.

Appendix A. Supporting information

Supplementary data associated with this article can be found in the online version at doi:10.1016/j.colsurfa.2021.127743.

References

[1] A. Pathak, P. Kumar, K. Chuttani, S. Jain, A.K. Mishra, S.P. Vyas, K.C. Gupta, Gene expression, biodistribution, and pharmacoscintigraphic evaluation of chondroitin sulfate−PEI nanoconstructs mediated tumor gene therapy, ACS Nano 3 (2009) 1493–1505, https://doi.org/10.1021/nn900044f.

[2] M. Thomas, A.M. Klibanov, Non-viral gene therapy: polycation-mediated DNA delivery, Appl. Microbiol. Biotechnol. 62 (2003) 27–34, https://doi.org/10.1007/s00253-003-1321-8.

[3] A.C. Nathwani, E.G. Tuddenham, S. Rangarajan, C. Rosales, J. McIntosh, D. C. Linch, P. Chowdary, A. Riddell, A.J. Pie, C. Harrington, J. O'Beirne, K. Smith, J. Pasi, B. Glader, P. Rustagi, C.Y. Ng, M.A. Kay, J. Zhou, Y. Spence, C.L. Morton, J. Allay, J. Coleman, S. Sleep, J.M. Cunningham, D. Srivastava, E. Basner-Tschakarjan, F. Mingozzi, K.A. High, J.T. Gray, U.M. Reiss, A.W. Nienhuis, A. M. Davidoff, Adenovirus-associated virus vector–mediated gene transfer in hemophilia B, N. Engl. J. Med. 365 (2011) 2357–2365, https://doi.org/10.1056/NEJMoa1108046.

[4] K. Banerjee, F.J. Núñez, S. Haase, B.L. McClellan, S.M. Faisal, S.V. Carney, J. Yu, M. S. Alghamri, A.S. Asad, A. Candia, M.L. Varela, M. Candolfi, P.R. Lowenstein, M. G. Castro, Current approaches for glioma gene therapy and virotherapy, Front. Mol. Neurosci. 14 (2021), 621831, https://doi.org/10.3389/fnmol.2021.621831.

[5] D. Cross, J.K. Burmester, Gene therapy for cancer treatment: past, present and future, Clin. Med. Res. 4 (2006) 218–227, https://doi.org/10.3121/cmr.4.3.218.

[6] H.Y. Nam, J.H. Park, K. Kim, I.C. Kwon, S.Y. Jeong, Lipid-based emulsion system as non-viral gene carriers, Arch. Pharmacal Res. 32 (2009) 639–646, https://doi.org/10.1007/s12272-009-1500-y.

[7] U. Lächelt, E. Wagner, Nucleic acid therapeutics using polyplexes: a Journey of 50 Years (and Beyond), Chem. Rev. 115 (2015) 11043–11078, https://doi.org/10.1021/cr5006793.

[8] C.L. Hardee, L.M. Arévalo-Soliz, B.D. Hornstein, L. Zechiedrich, Advances in non-viral DNA vectors for gene therapy, Genes 8 (2017), https://doi.org/10.3390/genes8020065.

[9] A.K. Levacic, S. Morys, S. Kempter, U. Lächelt, E. Wagner, Minicircle versus plasmid DNA delivery by receptor-targeted polyplexes, Hum. gene Ther. 28 (2017) 862–874, https://doi.org/10.1089/hum.2017.123.

[10] J. Zhao, P. Huang, Z. Wang, Y. Tan, X. Hou, L. Zhang, C.Y. He, Z.Y. Chen, Synthesis of Amphiphilic Poly(β-amino ester) for efficiently minicircle DNA delivery in vivo, ACS Appl. Mater. Interfaces 8 (2016) 19284–19290, https://doi.org/10.1021/acsami.6b04412.

[11] Z. Sohrabijam, M. Saeidifar, A. Zamanian, Enhancement of magnetofection efficiency using chitosan coated superparamagnetic iron oxide nanoparticles and calf thymus DNA, Colloids Surf., B 152 (2017) 169–175, https://doi.org/10.1016/j.colsurfb.2017.01.028.

[12] Y. Liu, Y. Tang, J. Wu, J. Sun, X. Liao, Z. Teng, G. Lu, Facile synthesis of biodegradable flower-like hydroxyapatite for drug and gene delivery, J. Colloid Interface Sci. 570 (2020) 402–410, https://doi.org/10.1016/j.jcis.2020.03.010.

[13] E. Fisicaro, C. Compari, F. Bacciottini, L. Contardi, E. Pongiluppi, N. Barbero, G. Viscardi, P. Quagliotto, G. Donofrio, M.P. Krafft, Nonviral gene-delivery by highly fluorinated gemini bispyridinium surfactant-based DNA nanoparticles, J. Colloid Interface Sci. 487 (2017) 182–191, https://doi.org/10.1016/j.jcis.2016.10.032.

[14] X. Lang, T. Wang, M. Sun, X. Chen, Y. Liu, Advances and applications of chitosan-based nanomaterials as oral delivery carriers: a review, Int. J. Biol. Macromol. 154 (2020) 433–445, https://doi.org/10.1016/j.ijbiomac.2020.03.148.

[15] E. Farris, D.M. Brown, A.E. Ramer-Tait, A.K. Pannier, Micro- and nanoparticulates for DNA vaccine delivery, Exp. Biol. Med. 241 (2016) 919–929, https://doi.org/10.1177/1535370216643771.

[16] R. Kandil, O.M. Merkel, Recent progress of polymeric nanogels for gene delivery, Curr. Opin. Colloid Interface Sci. 39 (2019) 11–23, https://doi.org/10.1016/j.cocis.2019.01.005.

[17] A.S. Piotrowski-Daspit, A.C. Kauffman, L.G. Bracaglia, W.M. Saltzman, Polymeric vehicles for nucleic acid delivery, Adv. Drug Deliv. Rev. 156 (2020) 119–132, https://doi.org/10.1016/j.addr.2020.06.014.

[18] C. Englert, J.C. Brendel, T.C. Majdanski, T. Yildirim, S. Schubert, M. Gottschaldt, N. Windhab, U.S. Schubert, Pharmapolymers in the 21st century: synthetic polymers in drug delivery applications, Prog. Polym. Sci. 87 (2018) 107–164, https://doi.org/10.1016/j.progpolymsci.2018.07.005.

[19] A. Rayegan, A. Allafchian, I. Abdolhosseini Sarsari, P. Kameli, Synthesis and characterization of basil seed mucilage coated Fe_3O_4 magnetic nanoparticles as a drug carrier for the controlled delivery of cephalexin, Int. J. Biol. Macromol. 113 (2018) 317–328, https://doi.org/10.1016/j.ijbiomac.2018.02.134.

[20] Z.R. Stephen, C.J. Dayringer, J.J. Lim, R.A. Revia, M.V. Halbert, M. Jeon, A. Bakthavatsalam, R.G. Ellenbogen, M. Zhang, Approach to rapid synthesis and functionalization of iron oxide nanoparticles for high gene transfection, ACS Appl. Mater. Interfaces 8 (2016) 6320–6328, https://doi.org/10.1021/acsami.5b10883.

[21] D. Wu, L. Zhu, Y. Li, X. Zhang, S. Xu, G. Yang, T. Delair, Chitosan-based colloidal polyelectrolyte complexes for drug delivery: a review, Carbohydr. Polym. 238 (2020), 116126, https://doi.org/10.1016/j.carbpol.2020.116126.

[22] S. Kumar, J. Dutta, P.K. Dutta, J. Koh, A systematic study on chitosan-liposome based systems for biomedical applications, Int. J. Biol. Macromol. 160 (2020) 470–481, https://doi.org/10.1016/j.ijbiomac.2020.05.192.

[23] B.N. Kumara, R. Shambhu, K.S. Prasad, Why chitosan could be apt candidate for glaucoma drug delivery - an overview, Int. J. Biol. Macromol. 176 (2021) 47–65, https://doi.org/10.1016/j.ijbiomac.2021.02.057.

[24] S.Y. Lee, J.S. Koo, M. Yang, H.-J. Cho, Application of temporary agglomeration of chitosan-coated nanoparticles for the treatment of lung metastasis of melanoma, J. Colloid Interface Sci. 544 (2019) 266–275, https://doi.org/10.1016/j.jcis.2019.02.092.

[25] H. Rahnama, S. Nouri Khorasani, A. Aminoroaya, M.R. Molavian, A. Allafchian, S. Khalili, Facile preparation of chitosan-dopamine-inulin aldehyde hydrogel for drug delivery application, Int. J. Biol. Macromol. 185 (2021) 716–724, https://doi.org/10.1016/j.ijbiomac.2021.06.199.

[26] L.M. Bravo-Anaya, K.G. Fernández-Solís, J. Rosselgong, J.L.E. Nano-Rodríguez, F. Carvajal, M. Rinaudo, Chitosan-DNA polyelectrolyte complex: influence of chitosan characteristics and mechanism of complex formation, Int. J. Biol. Macromol. 126 (2019) 1037–1049, https://doi.org/10.1016/j.ijbiomac.2019.01.008.

[27] Ö. Tezgel, A. Szarpak-Jankowska, A. Arnould, R. Auzély-Velty, I. Texier, Chitosan-lipid nanoparticles (CS-LNPs): application to siRNA delivery, J. Colloid Interface Sci. 510 (2018) 45–56, https://doi.org/10.1016/j.jcis.2017.09.045.

[28] L.M. Bravo-Anaya, J.F.A. Soltero, M. Rinaudo, DNA/chitosan electrostatic complex, Int. J. Biol. Macromol. 88 (2016) 345–353, https://doi.org/10.1016/j.ijbiomac.2016.03.035.

[29] Y. Liang, X. Zhao, P.X. Ma, B. Guo, Y. Du, X. Han, pH-responsive injectable hydrogels with mucosal adhesiveness based on chitosan-grafted-dihydrocaffeic acid and oxidized pullulan for localized drug delivery, J. Colloid Interface Sci. 536 (2019) 224–234, https://doi.org/10.1016/j.jcis.2018.10.056.

[30] F. Bordi, L. Chronopoulou, C. Palocci, F. Bomboi, A. Di Martino, N. Cifani, B. Pompili, F. Ascenzioni, S. Sennato, Chitosan–DNA complexes: effect of molecular parameters on the efficiency of delivery, Colloids Surf., A 460 (2014) 184–190, https://doi.org/10.1016/j.colsurfa.2013.12.022.

[31] D. Veilleux, R.K. Gopalakrishna Panicker, A. Chevrier, K. Biniecki, M. Lavertu, M. D. Buschmann, Lyophilisation and concentration of chitosan/siRNA polyplexes: influence of buffer composition, oligonucleotide sequence, and hyaluronic acid coating, J. Colloid Interface Sci. 512 (2018) 335–345, https://doi.org/10.1016/j.jcis.2017.09.084.

[32] S. Jaiswal, P.K. Dutta, S. Kumar, R. Chawla, Chitosan modified by organo-functionalities as an efficient nanoplatform for anti-cancer drug delivery process, J. Drug Deliv. Sci. Technol. 62 (2021), 102407, https://doi.org/10.1016/j.jddst.2021.102407.

[33] D. Njus, P.M. Kelley, Y.-J. Tu, H.B. Schlegel, Ascorbic acid: the chemistry underlying its antioxidant properties, Free Radic. Biol. Med. 159 (2020) 37–43, https://doi.org/10.1016/j.freeradbiomed.2020.07.013.

[34] A.M. Elbarbary, H.M. Shafik, N.H. Ebeid, S.M. Ayoub, S.H. Othman, Iodine-125 chitosan-vitamin C complex: preparation, characterization and application, Radiochim. Acta 103 (2015) 663–671, https://doi.org/10.1515/ract-2014-2303.
[35] J. Baek, M. Ramasamy, N.C. Willis, D.S. Kim, W.A. Anderson, K.C. Tam, Encapsulation and controlled release of vitamin C in modified cellulose nanocrystal/chitosan nanocapsules, Curr. Res. Food Sci. 4 (2021) 215–223, https://doi.org/10.1016/j.crfs.2021.03.010.
[36] H. Zou, Z. Wang, M. Feng, Nanocarriers with tunable surface properties to unblock bottlenecks in systemic drug and gene delivery, J. Control. Release 214 (2015) 121–133, https://doi.org/10.1016/j.jconrel.2015.07.014.
[37] E. Farris, K. Heck, A.T. Lampe, D.M. Brown, A.E. Ramer-Tait, A.K. Pannier, Oral non-viral gene delivery for applications in DNA vaccination and gene therapy, Curr. Opin. Biomed. Eng. 7 (2018) 51–57, https://doi.org/10.1016/j.cobme.2018.09.003.
[38] S. Massadeh, M. Al-Aamery, S. Bawazeer, O. AlAhmad, R. AlSubai, Nano-materials for gene therapy: an efficient way in overcoming challenges of gene delivery, J. Biosens. Bioelectron. 7 (2016) 1–12, https://doi.org/10.4172/2155-6210.1000195.
[39] G. Lin, L. Li, N. Panwar, J. Wang, S.C. Tjin, X. Wang, K.T. Yong, Non-viral gene therapy using multifunctional nanoparticles: status, challenges, and opportunities, Coord. Chem. Rev. 374 (2018) 133–152, https://doi.org/10.1016/j.ccr.2018.07.001.
[40] Q. Bi, X. Song, A. Hu, T. Luo, R. Jin, H. Ai, Y. Nie, Magnetofection: magic magnetic nanoparticles for efficient gene delivery, Chin. Chem. Lett. 31 (2020) 3041–3046, https://doi.org/10.1016/j.cclet.2020.07.030.
[41] A. Allafchian, S.S. Hosseini, Antibacterial magnetic nanoparticles for therapeutics: a review, IET Nanobiotechnol. 13 (2019) 786–799, https://doi.org/10.1049/iet-nbt.2019.0146.
[42] M.A. Busquets, A. Espargaró, R. Sabaté, J. Estelrich, Magnetic nanoparticles cross the blood-brain barrier: when physics rises to a challenge, Nanomater 5 (2015) 2231–2248, https://doi.org/10.3390/nano5042231.
[43] Q. Xu, T. Zhang, Q. Wang, X. Jiang, A. Li, Y. Li, T. Huang, F. Li, Y. Hu, D. Ling, J. Gao, Uniformly sized iron oxide nanoparticles for efficient gene delivery to mesenchymal stem cells, Int. J. Pharm. 552 (2018) 443–452, https://doi.org/10.1016/j.ijpharm.2018.10.023.
[44] R.P. Dhavale, P.P. Waifalkar, A. Sharma, R.P. Dhavale, S.C. Sahoo, P. Kollu, A. D. Chougale, D. Zahn, G. Salvan, P.S. Patil, P.B. Patil, Monolayer grafting of aminosilane on magnetic nanoparticles: an efficient approach for targeted drug delivery system, J. Colloid Interface Sci. 529 (2018) 415–425, https://doi.org/10.1016/j.jcis.2018.06.006.
[45] C. Saengruengrit, P. Ritprajak, S. Wanichwecharungruang, A. Sharma, G. Salvan, D. Zahn, N. Insin, The combined magnetic field and iron oxide-PLGA composite particles: effective protein antigen delivery and immune stimulation in dendritic cells, J. Colloid Interface Sci. 520 (2018) 101–111, https://doi.org/10.1016/j.jcis.2018.03.008.
[46] R. Hatami, A. Allafchian, F. Karimzadeh, M.H. Enayati, Preparation of amino silane magnetic nanocomposite by the sol–gel process and investigation of its antibacterial activity, Micro Nano Lett. 14 (2019) 196–201, https://doi.org/10.1049/mnl.2018.5491.
[47] E. Alphandéry, Iron oxide nanoparticles for therapeutic applications, Drug Discov. Today 25 (2020) 141–149, https://doi.org/10.1016/j.drudis.2019.09.020.
[48] O. Bezdorozhev, T. Kolodiazhnyi, O. Vasylkiv, Precipitation synthesis and magnetic properties of self-assembled magnetite-chitosan nanostructures, J. Magn. Magn. Mater. 428 (2017) 406–411, https://doi.org/10.1016/j.jmmm.2016.12.048.
[49] J.R. Sosa-Acosta, J.A. Silva, L. Fernández-Izquierdo, S. Díaz-Castañón, M. Ortiz, J. C. Zuaznabar-Gardona, A.M. Díaz-García, Iron oxide nanoparticles (IONPs) with potential applications in plasmid DNA isolation, Colloids Surf., A 545 (2018) 167–178, https://doi.org/10.1016/j.colsurfa.2018.02.062.
[50] N.A. Peppas, J.J. Sahlin, A simple equation for the description of solute release. III. coupling of diffusion and relaxation, Int. J. Pharm. 57 (1989) 169–172, https://doi.org/10.1016/0378-5173(89)90306-2.
[51] A.R. Allafchian, S.A.H. Jalali, S.E. Mousavi, Biocompatible biodegradable polycaprolactone/basil seed mucilage scaffold for cell culture, IET Nanobiotechnol. 12 (2018) 1108–1113, https://doi.org/10.1049/iet-nbt.2018.5071.
[52] A. Kumar, P.K. Jena, S. Behera, R.F. Lockey, S. Mohapatra, S. Mohapatra, Multifunctional magnetic nanoparticles for targeted delivery, Nanomed.: Nanotechnol., Biol. Med. 6 (2010) 64–69, https://doi.org/10.1016/j.nano.2009.04.002.
[53] M.-H. Ki, J.E. Kim, Y.N. Lee, S.M. Noh, S.W. An, H.J. Cho, D.D. Kim, Chitosan-Based Hybrid Nanocomplex for siRNA delivery and Its application for cancer therapy, Pharm. Res. 31 (2014) 3323–3334, https://doi.org/10.1007/s11095-014-1422-3.
[54] M. Lee, J.-W. Nah, Y. Kwon, J.J. Koh, K.S. Ko, S.W. Kim, Water-Soluble and low molecular weight chitosan-based plasmid DNA delivery, Pharm. Res. 18 (2001) 427–431, https://doi.org/10.1023/A:1011037807261.
[55] B.B.M. Garcia, O. Mertins, E.Rd Silva, P.D. Mathews, S.W. Han, Arginine-modified chitosan complexed with liposome systems for plasmid DNA delivery, Colloids Surf., B 193 (2020), 111131, https://doi.org/10.1016/j.colsurfb.2020.111131.
[56] Y.-L. Lo, H.L. Chou, Z.X. Liao, S.J. Huang, J.H. Ke, Y.S. Liu, C.C. Chiu, L.F. Wang, Chondroitin sulfate-polyethylenimine copolymer-coated superparamagnetic iron oxide nanoparticles as an efficient magneto-gene carrier for microRNA-encoding plasmid DNA delivery, Nanoscale 7 (2015) 8554–8565, https://doi.org/10.1039/C5NR01404B.
[57] S. Vimal, S. Abdul Majeed, K. Nambi, N. Madan, M.A. Farook, C. Venkatesan, G. Taju, S. Venu, R. Subburaj, A.R. Thirunavukkarasu, A.S. Sahul Hameed, Delivery of DNA vaccine using chitosan–tripolyphosphate (CS/TPP) nanoparticles in Asian sea bass, Lates calcarifer (Bloch, 1790) for protection against nodavirus infection, Aquaculture 420–421 (2014) 240–246, https://doi.org/10.1016/j.aquaculture.2013.11.017.
[58] S. Rodrigues, M. Dionísio, C.R. López, A. Grenha, Biocompatibility of Chitosan carriers with application in drug delivery, 615-41, J. Funct. Biomater. 3 (2012), https://doi.org/10.3390/jfb3030615.